Journal of Statistical Physics, Vol. 65, Nos. 3/4, 1991

Statistics of Two-Dimensional Point Vortices and High-Energy Vortex States

L. J. Campbell[1] and Kevin O'Neil[2]

Received December 18, 1990; final May 17, 1991

Results from the theory of U-statistics are used to characterize the microcanonical partition function of the N-vortex system in a rectangular region for large N, under various boundary conditions, and for neutral, asymptotically neutral, and nonneutral systems. Numerical estimates show that the limiting distribution is well matched in the region of major probability for N larger than 20. Implications for the thermodynamic limit are discussed. Vortex clustering is quantitatively studied via the average interaction energy between negative and positive vortices. Vortex states for which clustering is generic (in a statistical sense) are shown to result from two modeling processes: the approximation of a continuous inviscid fluid by point vortex configurations; and the modeling of the evolution of a continuous fluid at high Reynolds number by point vortex configurations, with the viscosity represented by the annihilation of close positive–negative vortex pairs. This last process, with the vortex dynamics replaced by a random walk, reproduces quite well the late-time features seen in spectral integration of the 2d Navier–Stokes equation.

KEY WORDS: Point vortices; microcanonical ensemble; negative temperature; thermodynamic limit; 2d turbulence; U-statistics.

1. INTRODUCTION

The statistics and accompanying thermodynamics of objects whose pairwise interaction energy in two dimensions is

$$v(\mathbf{r}_i, \mathbf{r}_j) = -\Gamma_i \Gamma_j \log |\mathbf{r}_i - \mathbf{r}_j|^2$$

have received much attention both for their intrinsic interest and their close representation of physical objects such as spin excitations, screw disloca-

[1] Theoretical Division, Los Alamos National Laboratory, Los Alamos, New Mexico 87545.
[2] Department of Mathematical and Computer Sciences, University of Tulsa, Oklahoma 74104-3189.

0022-4715/91/1100-0495$06.50/0

tions, line charges, guiding-center plasmas, superconducting fluxoids, and fluid vortices. Here, we are interested in fluid vortices and the structure of the microcanonical phase space associated with a periodic infinite lattice having N vortices with strengths Γ_i per unit cell. We also consider N vortices in a box (i.e., rigid walls), which is equivalent to correlated vortices in a periodic cell. Of particular interest are the statistical properties of vortices as the energy per vortex becomes large. This emphasis will be justified by showing how high-energy vortex states naturally arise from point vortex models of continuous vorticity.

Our results are both analytic and numerical. The existence of an asymptotic form of the microcanonical density of states at large N is established rigorously, while quantitative attributes are found numerically. Likewise, discussions of high-energy vortex states, such as the modeling of continuous flows and vortex clumping at high energy, use analytical arguments buttressed with numerical examples. Other parts are purely numerical, like the probability density of the average interaction energy between + and − vortices and the decay of high-Reynolds-number flow.

Onsager[1] observed that the boundedness of the total phase space of any finite number N of vortices implies that the volume of phase space per unit energy interval necessarily decreases for sufficiently high energy. The problem is to determine the thermodynamics, i.e., the limiting relationship between phase space and energy as $N \to \infty$ while the vortex density $N/A = \text{const}$. Negative temperature is implied by a phase space that decreases with energy, but Fröhlich and Ruelle give strong evidence that the formal thermodynamic limit of this system *eliminates* the negative-temperature region.[2] However, because the density of states of any finite vortex system has a maximum at finite energy, their result can be interpreted as showing the *absence* of a thermodynamic limit in the usual sense of a sufficiently large but finite system acquiring the intrinsic properties of the limiting infinite system. We show there is a unique probability density for the phase space that merely shifts to higher energy density, as N increases, by the amount $\log \sqrt{N}$.

In Section 2 we show analytically and by numerical estimate that for any combination of + and − vortices in a periodic unit cell a limiting probability density (of phase space) exists for the interaction component of the vortex energy density. Results for vortices in a box are similar, but differ in detail. In that part of the energy region accessible by random sampling this probability density has essentially converged for $N > 20$. Therefore, it is possible to consider the thermodynamics of the vortex lattice system with respect to this limiting probability density (by taking the logarithm to obtain the entropy). In this sense, a negative-temperature region does exist in the limit $N \to \infty$. This goes beyond the Salzberg–

Prager–May equation of state, whose derivation depends only on the form of the argument of the probability density, not its limiting properties.[3–5]

Characteristics of high-energy vortex states such as the interplay between high energy, high N, and total vorticity will be discussed in Section 3. An important consequence of the limiting probability density is the inevitable emergence of negative-temperature states when a vortex distribution, chosen to model a given continuous velocity distribution, is successively refined by increasing the number of vortices at constant total vorticity and constant total energy. Even though the probability density of the interaction energy per vortex quickly and uniformly converges as N increases, certain other characteristics, e.g., the average interaction between vortices of unlike sign, converge in a different fashion.

In Section 4 we employ the above results to model the decay of high-Reynolds-number fluids as a purely *statistical* process whereby an initial random distribution of point vortices is permitted to range over its constant-energy phase volume through a random walk. Viscosity is introduced by annihilating + and − vortex pairs that approach within a small distance. We find the salient features of such decay, such as the emergence of coherent vortex structures and their subsequent evolution to only two (of opposite vorticity) per unit cell, are reproduced by the statistical treatment. Associated phenomena, such as the development of the energy spectra, the overall relative loss of vorticity and energy, and the relative speed of these losses, also resemble results from direct integration of the Navier–Stokes equation by spectral techniques. The existence of a limiting probability density provides a justification for following the contraction in phase space (due to annihilation of vortex pairs) as the evolution of a single system. That system has the statistical property that the loss of vortex pairs reduces the total energy less than it increases the energy density of the remaining vortices, which are thereby driven deeper into the negative-temperature region, where the formation of well-separated regions of like-sign vorticity is generic.

Finally, a discussion and summary of the results appear in Section 5, including some checks on the accuracy of common approximations, such as the random-phase approximation and the sinh-Poisson equation.

2. VORTEX STATISTICS

The statistics of 2d point vortices has been studied exactly by Fröhlich and Ruelle[2] and approximately by several others, including Montgomery and Joyce,[6,7] Edwards and Taylor,[8] Seyler,[9] and Lundgren and Pointin[10–12]. Much of this is reviewed by Kraichnan and Montgomery.[5] With the help of U-statistics we obtain exact results which extend previous

work. Although we make no approximations, our numerical estimates are subject to random sampling error. While we have no disagreement with the results of ref. 2, we can now argue against an interpretation of those results that would deny an existence to negative temperatures for vortices. In fact, we emphasize the properties of the negative-temperature state. In general, the problems are reminiscent of, if less severe than, the 3d Coulomb case, which has been treated thoroughly.[13]

Here the system will be a periodic cell of area A containing N vortices with an energy per vortex $E(\mathbf{r}_1,..., \mathbf{r}_N)$. The microcanonical statistics is given by the distribution function $\Phi_N(\mathscr{E}, A)$, viz., the normalized volume of phase space with energy density $E(\mathbf{r}_1,..., \mathbf{r}_N)$ less than $\mathscr{E}/N$,

$$\Phi_N(\mathscr{E}, A) = \frac{1}{A^N} \int \cdots \int d\mathbf{r}_1 \cdots d\mathbf{r}_N \, \theta(\mathscr{E} - NE(\mathbf{r}_1,..., \mathbf{r}_N)) \tag{2.1}$$

where $\theta(x)$ is the step function. The probability density (partition function or structure function) is $\Omega_N = (\partial \Phi_N / \partial \mathscr{E})_A$, the entropy (ignoring correct Boltzmann counting as not relevant here) is $S(\mathscr{E}, A) = \kappa_B \log A^N \Omega_N$, and temperature $1/T = (\partial S / \partial \mathscr{E})_A$. These definitions acquire thermodynamic meaning if a limit exists for $N \to \infty$, $N/A = \text{const}$. While a limit does exist for vortices in a box, as shown by Fröhlich and Ruelle,[2] the convergence is *not* uniform, which reduces the usefulness of the associated thermodynamic properties inasmuch as they do not apply to *any* finite system over the entire range of $\mathscr{E}$. However, the convergence *is* uniform when a component of E corresponding to the interaction of a vortex with its periodic replicas (lattice) or images (box) is removed. This component is simply $(\log N)/2$.

Using Ewald methods[9] or similar procedures, one can write the lattice energy density (energy per vortex) as[14,15]

$$E(\mathbf{r}_1,..., \mathbf{r}_N) = \overline{\Gamma^2} \tilde{E} + \frac{\overline{\Gamma^2}}{2} \log\left(\frac{N}{D}\right) + e(\mathbf{r}_1,..., \mathbf{r}_N) \tag{2.2}$$

$$e(\mathbf{r}_1,..., \mathbf{r}_N) = \frac{1}{N} \sum_{i=1}^{N-1} \sum_{j=i+1}^{N} \Gamma_i \Gamma_j f(\mathbf{r}_i - \mathbf{r}_j; \mathbf{L}_1, \mathbf{L}_2) \tag{2.3}$$

where $\overline{\Gamma^2} = (1/N) \sum \Gamma_j^2$ and $\tilde{E}$ is a constant that depends on the shape but not the area of the unit cell (which has sides $\mathbf{L}_1$ and $\mathbf{L}_2$ and area $A = |\mathbf{L}_1 \times \mathbf{L}_2|$). The units of energy density E are $\rho\gamma^2/4\pi$, where ρ is the fluid mass per area and γ is the unit of circulation, length squared per time. It should be noted that (2.2) and its Ewald equivalent are derived by omitting the infinite energy associated with any nonneutrality of the system. The system consists of discrete vortices plus an inert, uniform, neutralizing

background, as needed. The lattice has a density $D = N/A$, and we will frequently take $|\Gamma_j| = 1$ and $D = 1$. It is sufficient to use the square unit cell, $|\mathbf{L}_1| = |\mathbf{L}_2| = L$, $\mathbf{L}_1 \perp \mathbf{L}_2$, for which $f(\mathbf{r})$ has the form $f(|x|/L, |y|/L)$. Therefore, the phase space for the vortex variables in f is the N-fold Cartesian product of the unit square, $0 \leqslant x_j/L, y_j/L < 1$. (Hereafter, when $\mathbf{r}$ appears as an argument of f it will be understood as $\mathbf{r}/L$.) Specifically, for the square unit cell,

$$\tilde{E} = \frac{\pi}{6} - \log\left\{2\pi \prod_{j=1}^{\infty} [1 - \exp(-2\pi j)]^2\right\} = -1.31053 \tag{2.4}$$

and

$$\begin{aligned} f(\mathbf{r}) &= f(x, y) \\ &= 2\pi\left[|y|(|y|-1) + \frac{1}{6}\right] \\ &\quad - \log\left\{\prod_{j=-\infty}^{\infty} [1 - 2\cos(2\pi x)\exp(-2\pi|j+y|) + \exp(-4\pi|j+y|)]\right\} \end{aligned} \tag{2.5}$$

Machine accuracy is achieved in the above products for $|j| \leqslant 5$.

In principle, it is straightforward to obtain a numerical picture of the probability density Ω_N in the region of $\mathscr{E}$ where $\Omega_N(\mathscr{E}, A)$ is maximum by counting the relative number of random configurations that have energy between equal intervals, where the vortex positions $\mathbf{r}_j$ are chosen independently and uniformly distributed over the unit square. That is, the density of states $\Omega_N(\mathscr{E}, A)$ can be found as the density function of the energy considered as a random variable, given independent, identically and uniformly distributed random vortex positions. The histograms so produced for Ω_N converge rapidly in shape but are shifted to larger energy by $N\overline{\Gamma^2}\log(N)/2$. This agrees with ref. 2, where it was proven that the slope of $\lim_{N\to\infty} \Omega_N(\mathscr{E}, A)$ is positive for all $\mathscr{E}$.

Extimates of such probability densities from 50,000 events for each N are plotted in Fig. 1. Different vortex sign mixtures are used and, to subtract the shift mentioned above, the results are given as a function of $e = E - \tilde{E} - (1/2)\log N$. To permit inspection of fluctuations relative to the number of events per energy interval, the probability density is not smoothed or normalized. The units are such that $E = \tilde{E} = -1.31053$ for any $N = p^2$ vortices on a square grid with spacing $1/p$, i.e., $e_{\text{square grid}} = -\log(N)/2$.

Not only does the probability density converge rapidly, but its con-

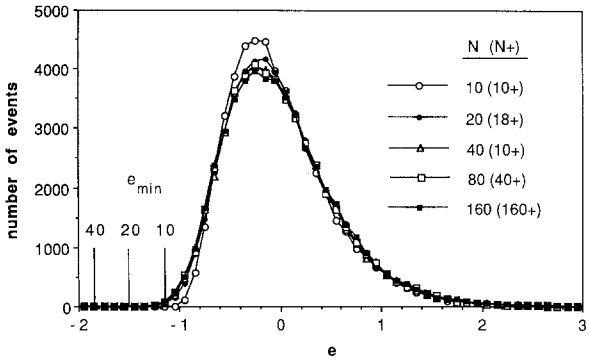

Fig. 1. Histogram of numerical probability density $\Omega_N(e)$ (unnormalized) for N vortices in a square periodic cell as a function of the interaction energy per vortex e. The total energy per vortex is $\tilde{E}+\log\sqrt{N}+e(\mathbf{r}_1,\ldots,\mathbf{r}_N)$. The magnitude of the vortex strengths is 1, but the signs are mixed as indicated in parentheses by the number of + vortices. The total number of events was 50,000 for each value of N. No smoothing was performed on this or subsequent data, with the exception of Figs. 9 and 16. The lower limit of finite probability density for $N=10$, 20, 40 vortices of the same sign is shown by the vertical lines.

vergent form is independent of the signs of Γ_j. This nonintuitive feature is a result of the existence of a limiting distribution for the random variable e and its particular form as a sum of correlated random variables.[16] For fixed N the probability density does depend on the signs of Γ_j, e.g., systems of equal-sign vortices have a lowest energy $e_{\min}=-\log(N)/2$, corresponding to the square lattice, while the energy of mixed sign systems is unbounded below. The bounds $e_{\min}$ are indicated in Fig. 1 for $N=10$, 20, and 40. However, these differences occur in a region of vanishing relative probability density and are of no concern here. Moreover, they disappear for fixed e as $N\to\infty$.

Because it is important for determining the type of probability density (normal versus nonnormal), we note that the integral of $f(\mathbf{r})$ over the unit cell, i.e., the expected value $\langle f\rangle$, is zero. This result follows from inspecting either the origins[9] of f or its implicit properties as a lattice interaction. We do the latter. If $m=p^2$ positive vortices are arranged on a regular square grid $\mathbf{g}_j$ in their periodic cell the energy per vortex $E(\mathbf{g}_1\cdots\mathbf{g}_m)$ is, by definition, the same as that for a single vortex in its periodic cell, $E(\mathbf{r}_1)$. Equating these energies as given by (2.2) gives

$$-\frac{1}{2}\log(m)=\frac{1}{m}\sum_{i<j}^{m}\sum f(\mathbf{g}_i-\mathbf{g}_j)=\frac{1}{2}\sum_{j=2}^{m} f(\mathbf{g}_1-\mathbf{g}_j) \tag{2.6}$$

where we used the equivalence of grid point differences. Let $\mathbf{g}_1$ be the origin and write the integral over the unit cell as

$$\iint d\mathbf{g}\, f(\mathbf{g}) = \lim_{m\to\infty} \frac{1}{m} \sum_{i=2}^{m} f(\mathbf{g}_i) = \lim_{m\to\infty} -\frac{1}{m}\log(m) = 0 \tag{2.7}$$

"Expected value" is a linear operator, so a simple corollary is

$$\langle e\rangle = \frac{1}{N} \sum_{i<j}^{N} \Gamma_i \Gamma_j \langle f(\mathbf{r}_i - \mathbf{r}_j)\rangle = 0 \tag{2.8}$$

Apart from the numerical evidence of Fig. 1, the existence of a limiting distribution for e follows from general theorems on "U-statistics." In particular, a U-statistic of degree two for symmetric kernel has the form

$$U_N(\mathbf{r}_1,\ldots,\mathbf{r}_N) = \frac{2}{N(N-1)} \sum_{i=1}^{N-1} \sum_{j=i+1}^{N} f(\mathbf{r}_i, \mathbf{r}_j) \tag{2.9}$$

It is known that if $\langle f^2\rangle < \infty$ and the expected value of $f(\mathbf{r}_1, \mathbf{r}_2)$ with respect to $\mathbf{r}_1$ is zero for all $\mathbf{r}_2$, then NU_N converges in distribution to a nonnormal distribution whose characteristic function is specified in terms of eigenvalues of f.[17] When all vortices have the same sign, e clearly has the form NU_N and $\langle f^2\rangle \approx \int \log(r)^2\, r\, dr < \infty$, so the theorem applies and, indeed, the probability density of Fig. 1 both converges and is nonnormal. The fact that e converges to the *same* distribution regardless of the sign mixture is a special feature of the form of e.[16] Moreover, using the methods of ref. 16, it can be shown that the magnitudes $|\Gamma_j|$ are also irrelevant; for arbitrary Γ_j the limiting distribution of $e/\overline{\Gamma^2}$ depends only on $f(\mathbf{r}_i, \mathbf{r}_j)$. Therefore, it is a convenience, not a restriction, to assume equal magnitudes for Γ_j.

The asymptotic distribution theory of U-statistics and related forms[17,16] seem to be little employed by the physics community, even though many statistical and thermodynamic quantities are naturally connected with these limiting distributions. For vortices, the existence of a limiting density of states with a stationary and well-defined maximum as a function of e allows us to speak of a statistical limit with respect to e, in which negative-temperature states exist (and, in fact, account for more than half of the volume of states in the system). With respect to the total energy per vortex, $E = E_0 + \log\sqrt{N} + e$, this maximum moves to infinity as N increases, giving a different statistical limit with no negative-temperature states.[2] The relevant physical point is that the $\log\sqrt{N}$ divergence is so slow that any particular system will have negative-temperature states at accessible energies.

Consider now vortices in a square box. As shown in Fig. 2, the box is equivalent to 1/4 of a periodic cell containing independent vortices and 3/4 of the cell containing dependent vortices. N vortices in the box give $4N$ vortices in the periodic cell at correlated positions. As a result, we may write for the box

$$e(\mathbf{r}_1,\ldots,\mathbf{r}_N)=\frac{1}{N}\left[\Gamma^2\sum_{i=1}^{N}b(\mathbf{r}_i)+\sum_{i=1}^{N-1}\sum_{j=i+1}^{N}\Gamma_i\Gamma_j h(\mathbf{r}_i,\mathbf{r}_j)\right] \tag{2.10}$$

where $b(\mathbf{r})$ is the interaction of a vortex with its own three images,

$$b(\mathbf{r})=\tfrac{1}{2}[-f(1-2x,0)-f(0,1-2y)+f(1-2x,1-2y)] \tag{2.11}$$

and $h(\mathbf{r}_1,\mathbf{r}_2)$ is the interaction between two vortices and their images,

$$\begin{aligned}h(\mathbf{r}_1,\mathbf{r}_2)=&f(|x_1-x_2|,|y_1-y_2|)-f(1-x_1-x_2,|y_1-y_2|)\\&-f(|x_1-x_2|,1-y_1-y_2)+f(1-x_1-x_2,1-y_1-y_2)\end{aligned} \tag{2.12}$$

An alternative and more compact expression for e in a box has been given in terms of Jacobi elliptic functions by Penna.[18]

To write e in terms of a U-statistic, let $\mu(r)=\int h(r,s)\,ds$, $\mu=\int\mu(r)\,dr$, and define

$$g(r_1,r_2)=h(r_1,r_2)-\mu(r_1)-\mu(r_2)+\mu \tag{2.13}$$

Now g is a degenerate kernel (i.e., $\iint g\,dr_1\,dr_2=0$), so the U-statistic $\tilde{e}=(1/N)\sum\Gamma_i\Gamma_j g(r_i,r_j)$ converges to a limiting distribution that is in general not normal. We have

$$e=\tilde{e}+\frac{\Gamma^2}{N}\sum b(r_i)+\frac{1}{N}\sum_{i<j}\Gamma_i\Gamma_j[\mu(r_i)+\mu(r_j)]-\frac{\mu}{N}\sum_{i<j}\Gamma_i\Gamma_j \tag{2.14}$$

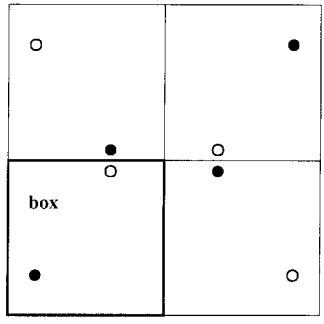

Fig. 2. Equivalence of box boundary conditions with a periodic cell four times as large. The filled and open circles represent vortices of opposite sign. Only the vortex positions in the box are independent.

Suppose that the distribution of unit circulations in the box is Nn_+ positive and Nn_- negative. Using the basic identity $(\sum \Gamma_i)^2 = \sum \Gamma_i^2 + 2\sum \Gamma_i \Gamma_j$ and setting $b(r_i) = b_i$, $\mu(r_i) = \mu_i$, we find

$$e = \tilde{e} + \Gamma^2 \frac{\mu}{2} + \frac{\Gamma^2}{N} \sum (b_i - \mu_i) + (n_+ - n_-)\,|\Gamma| \sum \Gamma_i \left(\mu_i - \frac{\mu}{2}\right) \tag{2.15}$$

For a neutral system the last sum in (2.15) vanishes, while the remaining sum tends to a constant with probability one, so the distribution of e tends to that of $\tilde{e}$ shifted by a constant. Thus, the statistical limit exists and is different from that of the system with periodic boundary conditions (although still nonnormal in general). Estimates of the neutral system probability density for various N are shown in Fig. 3. The convergence is rapid, as in Fig. 1, but the approach to convergence is different. The width is narrower than for the periodic cell and, as expected, the shape is nonnormal and the mode (maximum) occurs at lower energy.

Nonneutral systems in the box are qualitatively different. If $n_+ - n_- \neq 0$, the distribution of e is dominated by the rightmost term of (2.15), for which the central limit theorem implies the asymptotic distribution

$$\Omega_N(e) \sim \exp\left[- \frac{[e - (n_+ - n_-)^2 N\Gamma^2 \mu/2]^2}{2(n_+ - n_-)^2 N\Gamma^4 (\langle \mu_i^2 \rangle - \mu^2)} \right] \tag{2.16}$$

where $\langle \mu_i^2 \rangle - \mu^2 = \mathrm{Var}\, \mu_i$, the variance of μ_i. Thus, the total energy in the box Ne increases as N^2, ruling out a physical limit. Estimates of the probability density for all positive vortices are shown in Fig. 4. The

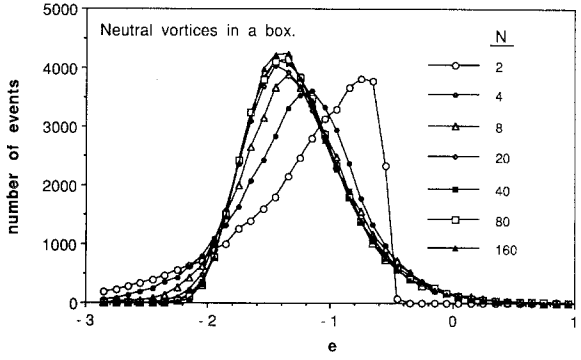

Fig. 3. Histogram of numerical probability density $\Omega_N(e)$ (unnormalized) for N vortices in a square box as a function of the interaction energy per vortex e. The numbers of + and − vortices are equal and the total number of events was 40,000 for each value of N.

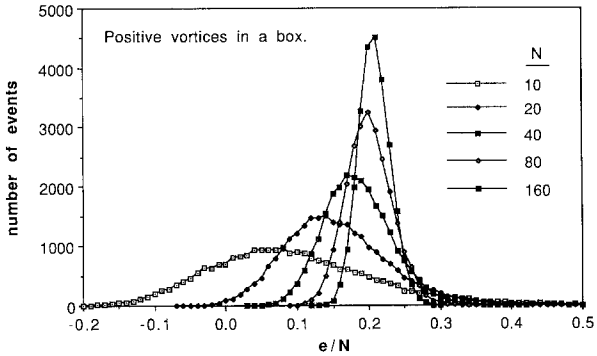

Fig. 4. Histogram of numerical probability density $\Omega_N(e)$ (unnormalized) for N positive vortices in a square box as a function of e/N. The total number of events was 25,000 for each value of N.

numerical convergence of the expected values is $\langle e_N/N \rangle = 2.20 - 15.34/N$. This case is discussed further in Section 5.

As can be seen from (2.15) and (2.16), there are two variants of nonneutral systems which have nontrivial statistical limits:

1. If the circulation imbalance is proportional to the perimeter of the box, $(n_+ - n_-)\sqrt{N} = c$, a constant, then the rightmost term of (2.15) no longer dominates, and the distribution for e is a mixture of normal and U-statistic with degenerate kernel. We found numerical evidence that the statistical limit again exists for this case, and a proof was constructed subsequently (K. A. O'Neil and R. A. Redner, to be published). This is analogous to the result found for surface charges on 3d Coulomb systems.[13] Estimates of the probability densities for various N and the edge or perimeter vorticity $(n_+ - n_-)\sqrt{N} = 3$ are shown in Fig. 5. The

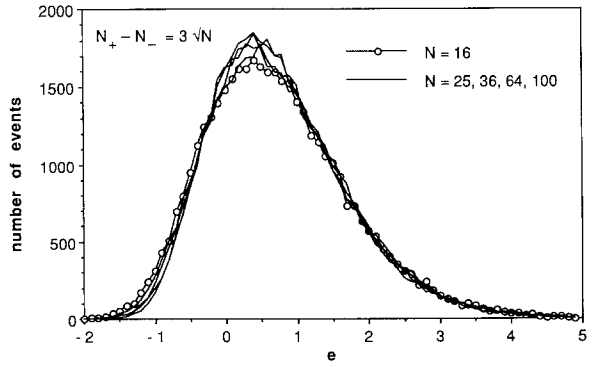

Fig. 5. Same as Fig. 3 except for *nonneutral* box systems having $(n_+ - n_-)\sqrt{N} = 3$, corresponding to a constant excess vorticity per unit of perimeter.

convergence is as rapid as before. By adjusting the amount of edge vorticity, it would seem possible to move $\langle e \rangle$ to any value greater than that for the neutral box system. (The existence of an "equation of state" in this case was noted by Hauge and Hemmer for positive temperature.[3])

2. Alternatively, if the vortex circulations are scaled with N as $\Gamma \to \Gamma_0/N$, a process we call "refinement," the resulting distribution of total energy has mean

$$\langle Ne \rangle = \tfrac{1}{2}(n_+ - n_-)^2 \Gamma_0^2 \iint h(\mathbf{r}_1, \mathbf{r}_2)\, d\mathbf{r}_1\, d\mathbf{r}_2 \tag{2.17}$$

and variance

$$\text{Var } Ne = (n_+ - n_-)^2 \frac{\Gamma_0^4}{N} (\langle \mu_i^2 \rangle - \mu^2) \tag{2.18}$$

That is, the energy tends to a point distribution, corresponding to the energy of fluid in a box with total vorticity $(n_+ - n_-)\Gamma_0$ and constant vorticity density. Refinement will be discussed further in the next section.

3. HIGH-ENERGY VORTEX STATES AND REFINEMENT

Having ensured the existence of a negative-temperature region for large N, let us consider some characteristics of that region, with emphasis on the periodic cell. We introduce a useful diagnostic for high-energy vortex states, discuss the statistical consequences of finely resolved vortex models of fluid flow, and mention numerical observations on high-energy vortex states.

Previous work on vortices in the negative-temperature region commonly found that a neutral system separated into clusters of opposite sign separated by a distance on the scale of the box or periodic cell. To quantify this effect in neutral systems, we introduce a statistical diagnostic of separation in the form of the average interaction energy between vortices of opposite sign,

$$\zeta_N = -\frac{4}{N^2} \sum_{i=1}^{N/2} \sum_{j=N/2+1}^{N} f(\mathbf{r}_i - \mathbf{r}_j) \tag{3.1}$$

where the first $N/2$ vortices are positive. The range of ζ_N is from $-\infty$ to $\zeta_{\max} = 0.693147 = f(\pm 0.5, \pm 0.5)$ for a square periodic cell. Near the maximum value, ζ_N indicates to first order the variance of the vortex distributions about the centers of the clusters, or the deviation of the centers from the limiting separation. (The existence of *two* clusters is special to neutral

systems, as shown later. Also, for box boundary conditions, image vortices prevent ζ_N from being a useful diagnostic.)

Consider the expected value of ζ_N conditional on $e = e_0$. From (2.3) the interaction energy of the neutral system, denoted e_{+-}, may be written,

$$e_{+-} = \frac{1}{N}\sum_{i<j}^{N+}\sum f(\mathbf{r}_i - \mathbf{r}_j) + \frac{1}{N}\sum_{i<j}^{N-}\sum f(\mathbf{r}_i - \mathbf{r}_j) - \frac{1}{N}\sum_{i=1}^{N+}\sum_{j=1}^{N-} f(\mathbf{r}_i - \mathbf{r}_j) \tag{3.2}$$

where $N+$, $N-$ refer to the sets of positive and negative vortices, respectively. This can be written in terms of ζ_N and the interaction energy e_{++} for N positive vortices by adding and subtracting the last term to obtain

$$e_{+-} = \frac{1}{N}\sum_{i<j}^{N}\sum f(\mathbf{r}_i - \mathbf{r}_j) + N\zeta_N/2 = e_{++} + N\zeta_N/2 \tag{3.3}$$

Recall that the unconditional averages are zero: $\langle e_{+-} \rangle = \langle e_{++} \rangle = 0$. Therefore, it is reasonable to suppose the weak conditional, $e_{+-} = e_0 \ll 1$, will affect e_{++} only in higher order, $\langle e_{++} \mid e_{+-} \rangle = e_0 \approx 0$. In that case, the conditional average value of ζ_N from (3.3) becomes

$$\zeta_N(e_0) \approx \frac{2e_0}{N} \tag{3.4}$$

This is a plausibility argument only. More thorough discussion of (3.4) and the fact that $N\zeta_N$ is also a U-statistic will not be pursued here.

In Fig. 6 we show numerical estimates for $\zeta_N(e)$, $N = 20$, 40, 80, as labeled. Also shown is $\Omega_{80}(e)$ for the same run of 20,000 events that

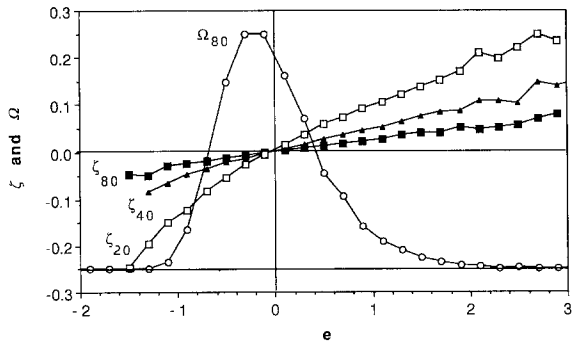

Fig. 6. Average interaction energy ζ_N between + and − vortices as a function of total interaction energy per vortex e. The values of $\zeta_N(e)$ are the average values appearing in the corresponding energy bins used for the histogram of the probability densities, only one of which is shown, for $N = 80$. Note the $\zeta_N(e)$ are linear, have slopes proportional to $1/N$, and have a common intersection at 0, the expected value of e.

produced the ζ_{80} data. These data were generated by finding the average value of ζ_N in each energy interval from random vortex configurations. The ζ_N curves are approximately linear and cross zero at $e=0$. The slopes obtained from numerical straight-line fits to the curves are $2.08/N$, $2.01/N$, and $2.13/N$ for $N=20$, 40, and 80, respectively, in reasonable agreement with (3.4).

Although Fig. 6 shows $\zeta_N(e)$ is linear for e near 0, it is impractical to generate data in this manner for $e>3$. Instead we use a random walk procedure which visits all the vortices in turn and moves each a random, but bounded, distance in the x and y directions. If the resulting step increases the energy, it is saved; otherwise not. Only one attempt is made per vortex in a cycle which visits all the vortices. In this way much higher energy states can be attained. Likewise, the statistical properties at a given energy can be explored by similar random steps that conserve the system's energy within an interval Δe. For example, $\zeta_N(e)$ can be estimated in this way at various e by averaging over all configurations visited by the random walk in a small energy interval about the target energy.

In Fig. 7, samples of $\zeta_N(e)$ for nine different random walk marches to high energy are shown, using $N=20$ (five curves) and $N=80$ (four curves). Also drawn is the linear relation $\zeta_N(e)=2e/N$ taken from Fig. 6; the fact that the random walk and the random sample results agree in the region of overlap gives confidence in the fairness of the random walk procedure. Note that the highest energies attained in Fig. 7 are $e\approx 30$ and 120 for $N=20$ and 80, respectively, far outside the random sampling region $|e|<3$. We wish to emphasize three features of the data in Fig. 7:

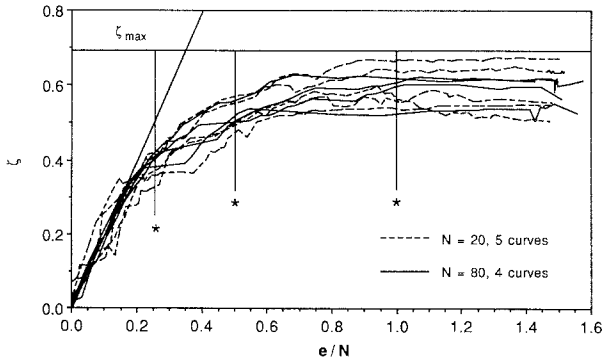

Fig. 7. Average interaction energy ζ_N between + and − vortices as a function of e/N. The ζ_N are the instantaneous values obtained during particular random walks to higher energy. Note that the $\zeta_N(e)$ agree with those obtained by random sampling in Fig. 6, from which the straight-line slope is taken. The vertical lines marked with asterisks are energy sections for probability densities of ζ_N shown in Fig. 9.

1. At high e, $\zeta_N(e)$ takes values near its maximum, indicating that most of the volume in phase space at high energies consists of configurations in which + and − vortices are separated into two clumps which have centers separated by $r = r_{max}$. To the extent that these values are estimates of $\zeta_N(e)$, the data in Fig. 7 allow us to predict the time average of the function ζ_N over the evolution of a typical configuration at high energies. Thus (assuming that the dynamics of point vortices are ergodic) for almost every initial configuration of vortices at high energy, the system will evolve by separation of the vortices into two clusters. Such behavior was indeed predicted by Onsager[1] and has been observed in many simulations in the past, but Fig. 7 represents the first quantitative statement about the *transition* to clusters to appear in the literature, to our knowledge. Furthermore, being statistical in nature, the information in Fig. 7 is quite general: a vortex system having the same phase space and interaction energy, and obeying *any* ergodic, energy-conserving dynamics, should have the same clustering behavior.

2. While all the curves are in close agreement for low e/N, the variance in the data increases with increasing e/N, and for large values the observed ζ_N range from near 0.35 to nearly the maximum of 0.7. All these configurations exhibit a high degree of clustering, but the centers of the clusters vary over a range of separations. This is because at high e/N the interaction between unlike vortices can add only a small fraction to the total interaction, which allows the separation to vary over a range. Consequently, the probability of ζ for two well-separated clusters is similar (but not identical, as shown below) to that of a two-vortex system, $\zeta_2 = -f(r)$, plotted in Fig. 8. Note the large probability between the interval of 0.3 and

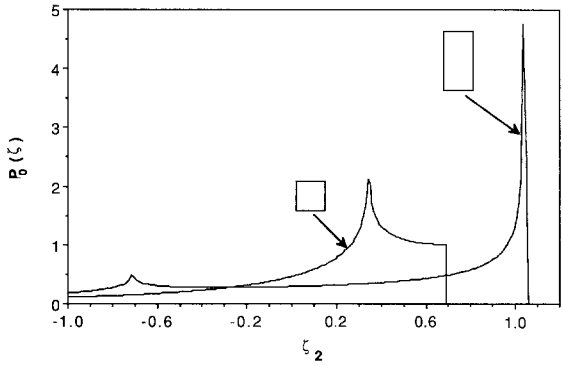

Fig. 8. Normalized probability density for $\zeta_2 = -f(\mathbf{r}_1 - \mathbf{r}_2)$ in square and rectangular periodic cells, as marked. This is also an important part of the probability density for ζ_N at high energy, where the vortices separate into two tight clusters of opposite sign.

0.7; this accounts for the observed spread of ζ_N at higher energies. Saddle points at $f(1/2, 0)$ and $f(0, 1/2)$ cause the cusp singularity. The shape of the unit cell influences the distribution probability of vortex clusters at high energy, just as the shape influences solutions to the sinh-Poisson equation.[19] This is illustrated in Fig. 8 by the probability density for a rectangular unit cell having $L_1 : L_2 = 1 : 2$.

3. The data suggest that $\zeta_N(e)$ is a function of e/N, and Fig. 7 uses e/N as the independent variable to highlight this relationship. This is consistent with the data in Fig. 6. One interesting consequence of this relationship is that for fixed e, the clustering of the vortex system *decreases* with increasing N. The suggestion that the cluster energy $\zeta_N(e)$ is a function of e/N is made more compelling by estimating the distribution of ζ_N for fixed e/N and different N. This is shown in Fig. 9 for $N = 20$ and 80, and $e/N = 0.25, 0.50$, and 1.0. Indeed, the modes of the distributions are equal for equal e/N. Also, the variance increases for larger e and decreases for larger N.

The high-energy behavior of ζ_N is further revealed by considering the joint probability,

$$P(\zeta, e) = \frac{1}{A^N} \int dr_1 \cdots dr_N \, \delta\left(\zeta + \frac{4}{N^2} \sum_{i=1}^{N/2} \sum_{j=N/2+1}^{N} f_{ij}\right) \times \delta\left(e - \frac{1}{N} \sum\sum_{i<j}^{N} f_{ij}\right) \tag{3.5}$$

For tight clusters the positive vortex positions are within a disk of radius R_+ centered at r_+; likewise for the negative vortices within R_- at r_-. The

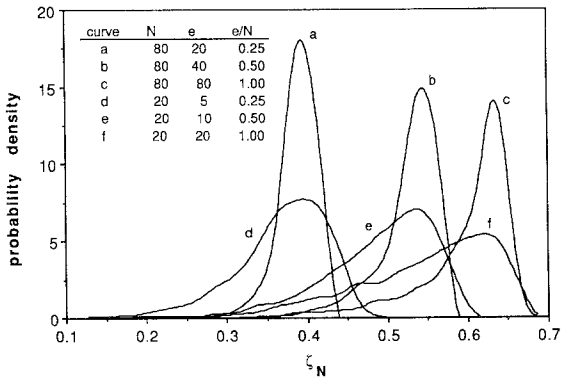

Fig. 9. Probability density (normalized and smoothed) of ζ_N at various fixed interaction energies e for $N = 20$ and 80. Each of these estimates is based on 5600 samples.

above integral can be approximated by introducing the coordinate $\mathbf{r}_+ - \mathbf{r}_-$ between clusters and taking all vortex coordinates relative to the center of their respective cluster, $\mathbf{r}_j - \mathbf{r}_\pm \to \mathbf{r}_j$. The first δ function in (3.5) becomes $\delta(\zeta + f(\mathbf{r}_+ - \mathbf{r}_-))$ and its integral (over $\mathbf{r}_+ - \mathbf{r}_-$) is just the probability density $P_0(\zeta)$ of Fig. 8. The remaining integral becomes

$$\frac{P(\zeta, e)}{P_0(\zeta)} = \frac{1}{A^N} \int dr_1 \cdots dr_N \, \delta\left(e - \frac{1}{N} \sum_{i<j}^{N+} \sum f_{ij} - \frac{1}{N} \sum_{i<j}^{N-} \sum f_{ij} - \frac{N}{4}\zeta\right) \tag{3.6}$$

It is convenient to write this as the derivative of a distribution function for the phase space volume corresponding to the cluster energies being *greater* than $e - N\zeta/4$,

$$\frac{P(\zeta, e)}{P_0(\zeta)} = -\frac{d}{de} \frac{1}{A^N} \int dr_1 \cdots dr_N \, \theta\left(-e + \frac{N}{4}\zeta + \frac{1}{N} \sum_{i<j}^{N+} \sum f_{ij} + \frac{1}{N} \sum_{i<j}^{N-} \sum f_{ij}\right) \tag{3.7}$$

The lowest energy E for M identical vortices in a small disk of radius R occurs when they are equally spaced on the circumference of the disk,

$$\begin{aligned} E(R) = \sum_{i<j}^{M} \sum f_{ij} &\approx -\sum_{i<j}^{M} \sum \log\left(\frac{|r_i - r_j|^2}{L^2}\right) + \frac{1}{2} M(M-1)\left(\frac{\pi}{3} - \log 4\pi^2\right) \\ &\approx -M^2\left(\log \frac{R}{L} + c\right) \end{aligned} \tag{3.8}$$

where the expansion of $f(r)$ from (2.5) for small r was used for the first line and the integral evaluation for the energy of the vortices on the circumference was used for the second line, in which $c = 1.314$. Therefore, the phase space of M vortices having higher energy than the ring is proportional to $(\pi R^2)^M$, corresponding to all possible positions of vortices in the disk. From (3.7) the minimum energy must be apportioned between the two disks; if the disk with N_+ vortices has minimum energy E_+, then the disk with N_- must have minimum energy $E_- = N(e - N\zeta/4) - E_+$. Then Eq. (3.7) becomes

$$\frac{P(\zeta, e)}{P_0(\zeta)} = -\frac{d}{de} \frac{1}{A^N} [\pi R_+^2 (E_+)]^{N+} \left[\pi R_-^2 \left(Ne - \frac{N^2\zeta}{4} - E_+\right)\right]^{N-} \tag{3.9}$$

Solving (3.8) for R gives

$$R(E) = L \exp\left(-\frac{E}{M^2} - c\right) \tag{3.10}$$

Substituting this into (3.9) and integrating over the energy partition, $0 \leqslant E_+ \leqslant N(e - N\zeta/4)$, gives the relative probability,

$$P(\zeta, e) = P_0(\zeta) \frac{[\pi \exp(-2c)]^N}{1/N_- - 1/N_+} \left(\frac{1}{N_+} \exp\left[-\frac{2N}{N_+}\left(e - \frac{N\zeta}{4}\right)\right] - \frac{1}{N_-} \exp\left[-\frac{2N}{N_-}\left(e - \frac{N\zeta}{4}\right)\right]\right) \tag{3.11}$$

For the neutral system, $P(\zeta, e) \sim P_0(\zeta) \exp(-4e + N\zeta)$, which shows a strong preference for the largest possible cluster separation (i.e., largest ζ) when N is large. For $e \gg N\zeta/4$ only the term associated with the majority species remains significant in (3.11), which is equivalent to saying that only configurations that preserve the majority cluster are statistically significant: *only one cluster occurs in the most probable states of high energy, nonneutral systems*, viz., the cluster for the majority species. To our knowledge this basic property of vortex systems has not previously been noted. (A shorter derivation is given in Section 5.) The same argument diminishes the probability of multiple clusters in high-energy systems of one sign.

We now demonstrate that using vortices to model a continuous inviscid fluid results in configurations having high e. By "model" we mean the following: given the initial condition of the continuous fluid in the periodic cell, one constructs a point vortex configuration that approximates the given vorticity distribution. Since the point vortex system is a singular solution of the Euler equations, the evolution of the (finite-dimensional) point vortex system should approximate the evolution of the (infinite-dimensional) continuous system, at least for some interval of time. The larger the number of point vortices in the system, the more accurately the continuous vorticity distribution is simulated, and the longer the interval; see Goodman *et al.*[20] for related convergence results. (Because the Euler equations excite arbitrarily small scales, the systems must eventually diverge.)

Assume as given the continuous initial velocity field v, vorticity distribution ω, and total kinetic energy W for the fluid in the periodic cell. It is convenient to break ω into its positive and negative parts, $\omega_\pm = \omega\theta(\pm\omega)$, so that $\omega = \omega_+ + \omega_-$. As usual we assume that the total vorticity in the periodic box is zero, $\int \omega_+ = -\int \omega_-$. Let $\Gamma = \int |\omega|$, and pick a large even integer N. Consider the system of N point vortices, half with circulation Γ/N and half with $-\Gamma/N$. Choose positions for the + and − vortices so as to approximate ω_+ and ω_-, respectively. For example, approximate ω by a step function $\tilde{\omega}$, and then place point vortices in a regular pattern at the appropriate densities in the level sets of $\tilde{\omega}$. This is

far from a unique specification, but we will see that the details of the configuration are unimportant, so long as the point vortices are not placed too close together.

Consider the energy of this configuration. Because the vortices are being subdivided in a constant area A, (2.2) must be generalized to include a general core energy per vortex, $\varepsilon = \Gamma^2 c_1 \log c_2 N$, where c_j are constants. Then, the total kinetic energy of the fluid inside the periodic cell is (substituting Γ/N for Γ in ε),

$$W_N = \frac{\Gamma^2}{N}(\tilde{E} + c_3 \log N + c_4 + e_N) \tag{3.12}$$

In accordance with previous usage, the quantity e_N has been computed with circulations of absolute value 1. (For this reason, we shall not refer to e_N as "energy density" in this section.) Clearly in the limit of large N the logarithm term vanishes and we have $W_N \to \Gamma^2 e_N/N$. On the other hand, the double summation $\Gamma^2 e_N/N = N^{-2} \sum\sum \Gamma_i \Gamma_j f(\mathbf{r}_i - \mathbf{r}_j)$ is an approximation of the Lamb energy integral

$$\iint \omega(\mathbf{r}_1)\, \omega(\mathbf{r}_2)\, f(\mathbf{r}_1 - \mathbf{r}_2)\, d\mathbf{r}_1\, d\mathbf{r}_2 \tag{3.13}$$

which equals the energy W. Thus, in the limit of large N, we find $e_N \to NW/\Gamma^2$, and the configurations used to model the continuous flow have very large values of e and therefore lie deep in the negative-temperature region. It is interesting that the configurations needed to simulate realistic (i.e., continuous) fluid flow are exactly those which are excluded from the formal thermodynamic limit!

There is a further regularity about these configurations which gives some insight into the statistics of the continuous fluid system. In this we make contact with recent work by Miller.[21] For large N, the configurations have the same value of e_N/N, namely W/Γ^2, and by Fig. 7 all have the same expected value for the separation function ζ_N. But this function in turn is an approximation to a variant of the Lamb integral,

$$\begin{aligned} \zeta &= \frac{4}{\Gamma^2} \iint \omega_+(\mathbf{r}_1)\, \omega_-(\mathbf{r}_2)\, f(\mathbf{r}_1 - \mathbf{r}_2)\, d\mathbf{r}_1\, d\mathbf{r}_2 \\ &= \iint \left(\frac{\omega_+(\mathbf{r}_1)}{\Gamma/2}\right)\left(\frac{\omega_-(\mathbf{r}_2)}{\Gamma/2}\right) f(\mathbf{r}_1 - \mathbf{r}_2)\, d\mathbf{r}_1\, d\mathbf{r}_2 \end{aligned} \tag{3.14}$$

(Recall that $\int \omega_+ = -\int \omega_- = \Gamma/2$.) Clearly this integral gives the same information as the discrete ζ_N, taking its maximum at the degenerate con-

figuration of two-point concentrations of vorticity, and indicating by nearness to this maximum the degree of separation of the vorticity of opposite senses in the unit cell. Taking the limit $N \to \infty$, we arrive at the conclusion that the integral ζ will have the time average predicted by Fig. 7, taking W/Γ^2 for e/N. (The quantity W/Γ^2 represents the energy of the fluid after rescaling the velocity field to make $\Gamma = 1$.)

Several points deserve emphasis. First, the normalized energy W/Γ^2 is positive, so our model predicts a positive value for the average of ζ. Second, if the initial condition of the fluid makes this normalized energy large, then the emergence of two maximally separated coherent vortices is a statistical phenomenon, applying to any system with the same state space, interaction energy, and ergodic dynamics. The emergence of these vortices is commonly observed in simulations of the relaxation of fluids at high Reynolds numbers; such effects of viscosity are discussed in the next section. Finally, we note that while our finite-dimensional point vortex systems cannot simulate the arbitrarily fine scales which are excited by the Euler equations, we find that all sufficiently resolved point vortex systems compatible with the continuous fluid system give the same prediction of this coarsest scale of motion, which simulations have shown to dominate the flow.

To further illustrate the previous discussion, Fig. 10a shows a neutral initial state consisting of 200 vortices in several tight clusters (so tight that most vortex symbols are hidden by overlap). Figure 10b shows the evolution of this initial state to the expected two-cluster state using a random walk at constant energy $e = 112$ within an interval $\Delta e < 0.02e$. The generic probable state in Fig. 10b agrees with the stable continuum state Carnevale

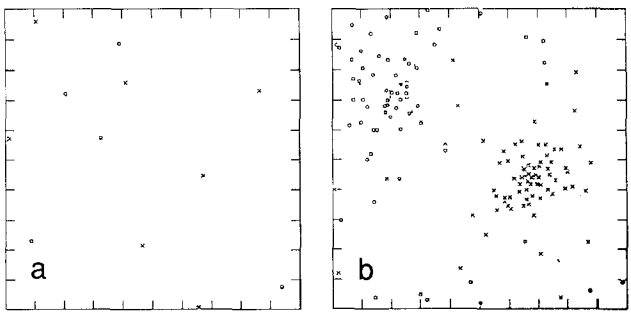

Fig. 10. Configurations of 200 vortices (equal numbers of + and −) having $e = 112$ in a periodic cell of side L. (a) Length of random step $\leqslant 0.05L$. (Most vortices are hidden by overlap in the tight clusters.) (b) Length of random step $\leqslant 0.4L$. Pattern (a) was generated by accepting only higher-energy steps starting from a low-energy random distribution. Pattern (b) evolved from (a) by random steps at constant energy ($\pm 2\%$).

and Vallis find by quite different methods: maximizing energy while keeping the system on an isovortical sheet.[22] In addition, Fig. 10a illustrates the bias introduced by a small step size: this highly improbable state was produced by a random march from an initially low-energy, random configuration by using a maximum step size of only $0.05L$. The more probable state in Fig. 10b was obtained from Fig. 10a in about 5000 steps with a maximum step size of $0.4L$. If the smaller step size had been used to evolve Fig. 10a at constant energy, the same final state would have been obtained through drift and merger of the tight clusters, but only after far more steps. (The probable configuration in Fig. 10b could have been obtained directly by using the larger step size to march the low-energy configuration to higher energy.)

High-energy vortex states in a box show distinct differences from those in a periodic cell. Although a random walk from an initial random configuration to higher energy, as described above, leads always to two well-defined, separated clusters of opposite sign, as occurs in the periodic cell, this seems not to be the most probable distribution. Further random steps at the fixed high energy causes one of the clusters to break up and spread around the boundary while the other cluster moves toward the center of the box and becomes even more compact than initially. For a nonneutral system the compact cluster is the majority species. The average intervortex spacing $\Delta r_{\pm}$ among vortices of equal sign reveals this evolution in Fig. 11. This behavior is suggestive of the solution to the sinh-Poisson equation that has a single extremum.[10] Vortex clusters corresponding to other solutions of the sinh-Poisson equation, such as four equal clusters on a

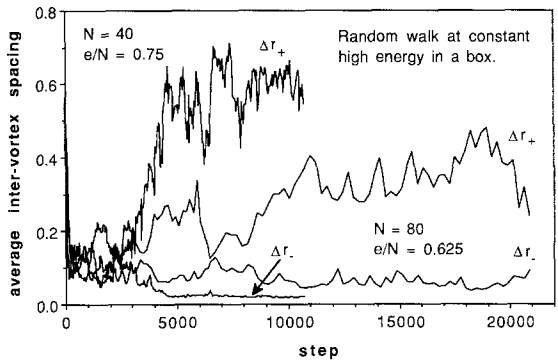

Fig. 11. Average intervortex separations among positive vortices Δr_+ and negative vortices Δr_- in a box as a function of the number of random steps constrained by fixed energy e. Two cases are shown: $N=40, e=30$ and $N=80$, $e=50$. The initial state consisted of two well-defined clusters for which $\Delta r_+ \approx \Delta r_-$. Random steps at constant energy cause one cluster to spread and the other to shrink.

checkerboard, were put in "by hand" and allowed to evolve at constant energy. These, too, tended to break up into one well-defined cluster and a diffuse collection of the opposite sign nearer the boundary, consistent with the instability of similar sinh-Poisson solutions.[11] The number of steps needed for this evolution to occur becomes much greater at higher energy, making impossible any conclusion from the numerical evidence that the same final state occurs at arbitrarily high energy. Also, the final state may be different in boxes with aspect ratio different from 1.

4. RELAXATION OF HIGH-REYNOLDS-NUMBER FLUIDS TO HIGH-ENERGY VORTEX STATES

In the previous section it was shown how increasing the number of vortices at constant total energy and vorticity led to negative-temperature states; here we show how a system is driven to negative temperatures by the dissipative loss of vorticity. No dynamical equation is employed; as a result we can say nothing about the flow apart from statistical properties. This is a different and more restricted vortex model of dissipative behavior than that of Chorin, in which vortex motion is based on advection with the local stream velocity plus a random component with variance proportional to the time step divided by the Reynolds number.[23]

As pointed out by Kraichnan and Montgomery,[5] turbulent flows are out of equilibrium in two respects: the macroscopic excitation of hydrodynamic modes is a departure from thermodynamic equilibrium with any heat bath and the hydrodynamic modes are typically in disequilibrium among themselves. The former disequilibrium we treat by allowing any pair of opposite-sign vortices to self-annihilate if they are sufficiently close; a prescription based on the known concentration of viscous dissipation at short distances for large Reynolds number. (Of course, there is no point in explicitly balancing the lost kinetic flow energy with added heat in the fluid unless important flow parameters such as viscosity or density are changed by a rise in fluid temperature.) The latter disequilibrium we treat statistically by performing a random walk over vortex configurations at constant energy (between e and $e + \Delta e$). In this way the vortex configuration moves, apart from fluctuations, from improbable (disequilibrium) to probable (equilibrium) configurations, as illustrated in the evolution of Fig. 10a to Fig. 10b. When a vortex pair disappears the remaining configuration is typically left in a relatively improbable state and adjusts over subsequent random steps.

We start with a neutral configuration of vortices randomly placed in the square periodic cell. Goodman, Hou, and Lowengrub proved that the

point vortex approximation to the 2d incompressible Euler equations enjoys consistency, stability, and convergence.[20] Therefore, we might expect statistical flow properties of the Eulerian fluid to be well-approximated by vortex dynamics. If the vortex system is ergodic, then the statistical properties can be obtained by averages over phase space instead of time averages of the dynamical equations. Although the ergodicity of the vortex system has been recently questioned[24] on the basis of numerical results for six vortices, we explore the consequences of relying on phase space averaging to obtain statistical behavior for a number of vortices sufficiently large to fairly represent the convergent probability distribution. For this, six vortices are too few by a significant factor.

In particular, we generate a random vortex configuration and use a random walk at constant energy to generate subsequent vortex configurations. A small viscosity is introduced by annihilating, in the course of the random walk, any pair of opposite-sign vortices that become sufficiently close. As mentioned above, this reflects the well-known dominance of dissipation at high wave numbers in high-Reynolds-number fluid flow and the attending cancellation of opposite vorticities at short distances. On larger distance scales the high-Reynolds-number fluid is inertial, i.e., Eulerian, and here the random walk at constant energy continues to rearrange the vortex configurations until other opposite pairs become close and are annihilated.

Besides reducing the number of vortices, pair annihilation increases the energy per vortex of the remaining vortices (because the energy of the lost pair is negative), but only weakly decreases the total energy NE_N, especially in the late stages. The persistent loss of close $+-$ pairs increases the average separation between the remaining $+$ and $-$ vortices and consequently increases the average interaction energy, i.e., the vortex separation energy ζ_N increases. Thus, the effect of annihilating pairs in response to weak viscosity is to drive the system deeply into the negative-temperature region. Close encounters of $+-$ vortices are initially quite frequent (in terms of the number of random steps between annihilations), but become relatively rare when well-defined vortex concentrations begin to emerge in the manner found by McWilliams from integrating the Navier–Stokes equations.[25] If the random walk is continued for much longer "times," the local vortex concentrations eventually become concentrated in two global clusters of opposite sign, quite similar to that found in the long integration runs by Matthaeus *et al.*[26]

The above behavior is illustrated in the Figs. 12–14 for a typical evolution of 200 vortices starting from a random configuration with $e = 5$, which was achieved by first marching a lower energy random configuration to higher energy (as described in the previous section) before starting the

relaxation. (This procedure merely saves time; the relaxation of some larger number of vortices starting at lower energy e would pass close to $N=200$ and $e=5$.)

Figure 12 shows the evolution of the $+-$ vortex interaction energy ζ, the number of vortices N, and the total energy $NE(N)$. (The last two are normalized with respect to their initial values.) The number of steps count only those random steps for which the energy falls within the interval Δe about e. (Here, $\Delta e=0.2$.) Following an annihilation of a $+-$ pair, the interaction energy density e increases, but Δe is held constant. The total energy decreases much less than the number of vortices, especially in the last two decades of the four-decade interval, where the interaction energy ζ rises to near its limit.

Streamlines of the system at steps 1, 161, 921, and 8521, corresponding to $N=200$, 100, 50, and 32, are shown in Fig. 13 with a resolution of 128×128. The resolution of vortex positions was 1024×1024; relaxation runs using higher resolution, 2000×2000, exhibited no observable difference for 200 vortices. The criterion for annihilation was a $+-$ pair separation (modulo L) of both Δx and $\Delta y\leqslant0.05L$, where L is the dimension of the periodic cell. The value of the annihilation distance is not critical; it should be small enough to permit several equilibrating steps between annihilations and large enough to permit an observable rate of annihilation. As might be expected from the absence of dynamics, there is no obvious filimentary structure associated with regions of concentrated vorticity, as seen from numerical simulations using the Navier–Stokes equation.[25,26] Also, the streamlines show numerous small-scale deflections

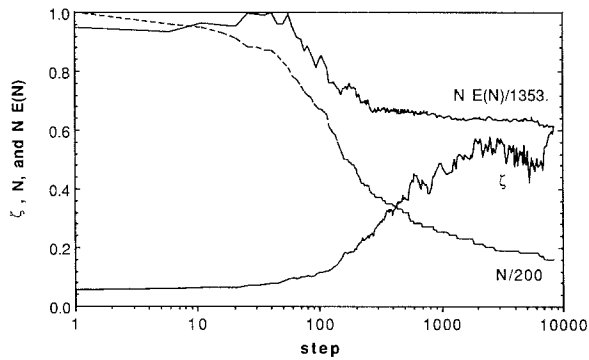

Fig. 12. System parameters during the viscous relaxation of 200 vortices (equal numbers of + and −) with an initial energy $e=5$. Each step is a random vortex displacement that preserves the energy density e within de. The system parameters change whenever a $+-$ vortex pair becomes sufficiently close to be annihilated due to viscosity.

as a result of the high velocities near point vortices, even though the vortex velocities were smoothed over a grid size $1/128 \times 1/128$ corresponding to the resolution. As can be seen in Fig. 13, the initially chaotic state becomes progressively differentiated into regions of like-sign vorticity, leading finally to two regions maximally separated on the diagonal like that found by Matthaeus *et al.*[26]

The modal energy spectra $E(k)$ corresponding to the streamlines in Fig. 13 are shown in Fig. 14. ($\int E(k)\, dk$ is proportional to the total energy.)

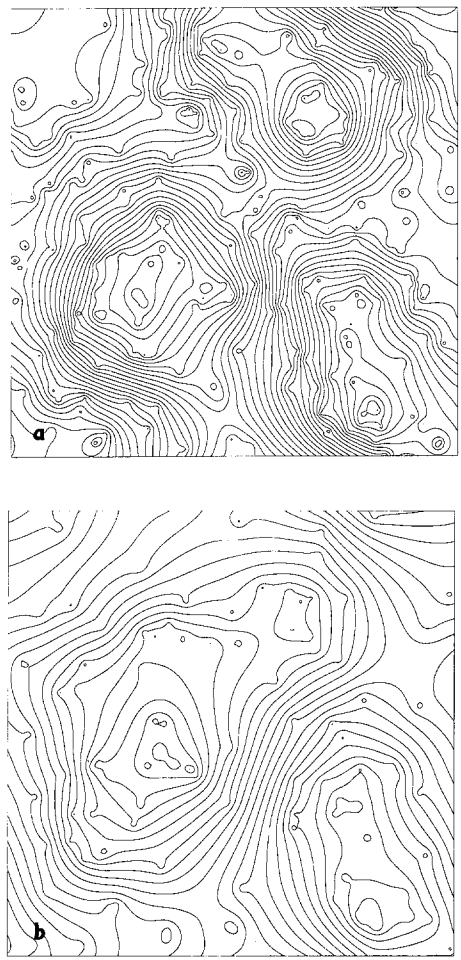

Fig. 13. Streamlines corresponding to the viscous relaxation of Fig. 12. (a) $N = 200$, step $= 0$; (b) $N = 100$, step $= 161$; (c) $N = 50$, step $= 921$; (d) $N = 32$, step $= 8521$.

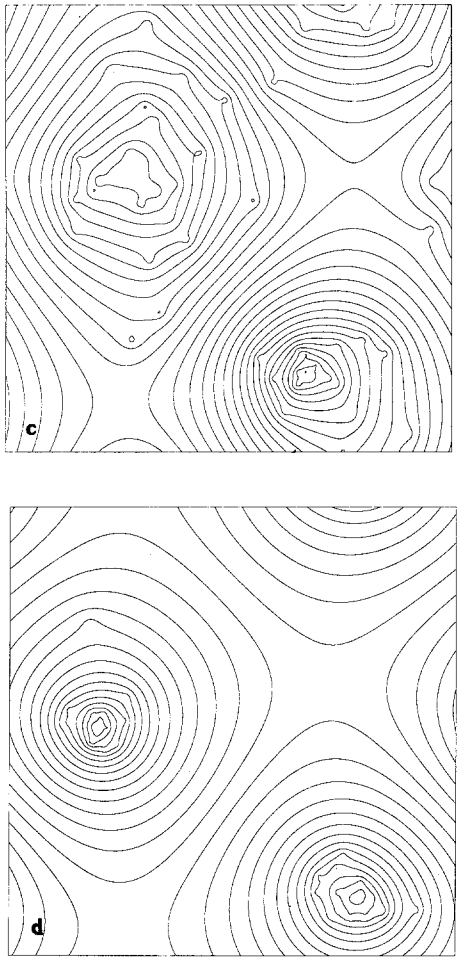

Fig. 13. (*Continued*)

Unlike the case of continuous vorticity, point vortices cause the high k values of $E(k)$ to remain large at all stages. In the last stage, $N=32$, the energy spectrum at low k is very close to that of two vortices with circulations $\Gamma = \pm 16$, shown by the solid curve without symbols. The trend is for energy to increase in the lowest modes and to decrease in the highest, as seen in spectral calculations.

The relaxation so far described is, of course, only an intermediate state in the viscous relaxation to total quiescence. Although we have not attempted it, further relaxation to any desired level of remnant vorticity is possible by successive refinement of the vorticity, as described in the pre-

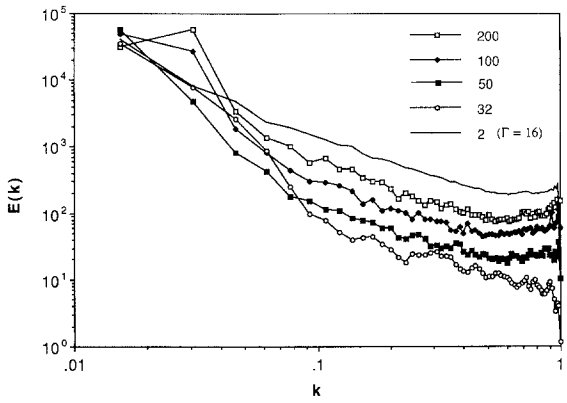

Fig. 14. Energy spectra corresponding to the streamlines of Fig. 13.

vious section, followed by the same prescription of vortex-pair annihilation. In this way even the essentially laminar late stage of the initial turbulent state, as represented by Fig. 13d, may be followed, in principle, to its linear viscous end, although the evolution should be quite different from that starting from a turbulent state. However, it remains to be seen if the statistical description of laminar decay can be as successful as that of turbulent decay. Because there is no inertial range in laminar decay, the approximation made here of confining viscous effects to the annihilation of $+-$ vorticity at a fixed distance would be questionable.

5. DISCUSSION

The statistical theory of vortex systems is well-founded. By this we mean that, as $N \to \infty$, there exist rigorous limiting probability densities of phase space volume as a function of the interaction energy per vortex e. These exist both for the periodic cell containing vortices of arbitrary signs (and strengths) and for the box containing neutral as well as special cases of nonneutral vortices (finite vorticity proportional to the box perimeter or constant vorticity under refinement). In every case the probability density has a mode at finite e, which defines the boundary between regions of positive and negative temperature, independent of vortex number. The expected values $\langle e \rangle$ for vortices in a periodic cell and neutral vortices in a box both occur at *negative* temperature. These results are summarized in Table I. We believe Table I lists *all* the possible limiting distributions of 2d point vortices in a periodic cell or box. Many properties of the U-statistic distributions remain to be calculated.

Table I

System	$\langle e \rangle$ [expected value]	$e_{\max}$ [mode of $\Omega(e)$]	Fwhm[a] or variance	Character of $\Omega(e)$ [distribution function]
Periodic cell, arbitrary $+-$ vortex mixture (numerical estimate)	0	-0.255 ± 0.005	fwhm $= 1.13 \pm 0.05$	Skewed, U-statistic with degenerate kernel
Box, neutral mixture (numerical estimate)	-1.258 ± 0.001	-1.40 ± 0.03	fwhm $= 0.85 \pm 0.05$	Skewed, U-statistic with degenerate kernel
Box, $N_+ - N_- = c\sqrt{N}$, constant surface vorticity	Increases with c	Increases with c	Increases with c	Skewed, sum of U-statistic and normal
Box, n_+, n_- fractions (Nn_+ positive and Nn_- negative vortices)	$(n_+ - n_-)^2 N\Gamma^2\mu/2$	$\langle e \rangle$	Var $e \equiv \sigma^2$ $= (n_+ - n_-)^2 N\Gamma^4 \times (\langle \mu_i^2 \rangle - \mu^2)$	Standard normal: $\mathcal{N}(\langle e \rangle, \sigma^2)$
Box, $n_+ = 1$ (numerical estimate)	$\langle e/N \rangle \to 2.20 \pm 0.01$	$\langle e/N \rangle$	Var $e/N \to 0$	Normal
Box, n_+, n_- fractions with refinement: $\Gamma = \Gamma_0/N$	$\langle Ne \rangle = (n_+ - n_-)^2 \Gamma_0^2 \mu/2$	$\langle Ne \rangle$	Var $Ne \equiv \sigma^2$ $= (n_+ - n_-)^2 \Gamma_0^4/N \times (\langle \mu_i^2 \rangle - \mu^2)$	$\Omega_N(Ne) = \mathcal{N}(\langle Ne \rangle, \sigma^2)$

[a] Full width at half-maximum.

A generally accepted physical assumption for vortex systems is that "the thermodynamic limit is a good approximation for the description of large, finite systems at moderate densities and energies."[2] The work here shows this assumption cannot be extended to high energies because the generic negative-temperature state that occurs in every large, finite system is missed by the formal, nonuniformly convergent limit with respect to the total energy density E_N. We further show that the requisite energies for the negative-temperature region are easily achieved in the course of approximating continuous vorticity by discrete vortices either as an initial condition (to be evolved by some method) or as a statistical model for the relaxation of a high-Reynolds-number fluid.

By identifying the energy density as a U-statistic of degree two, the rigorous existence and construction theorems from mathematical statistics[17,16] concerning limiting distributions can be used with a considerable savings of effort compared with *ab initio* approaches.[2] We made use only of the existence theorems here. However, procedures are known[17] for constructing the characteristic functions for distributions of U-statistics from the eigenvalues of the kernel.

Our calculations of probability densities are based on direct estimates from random sampling, rather than construction mentioned above. Nevertheless, we believe they are accurate within the errors listed in Table I, which are sufficiently small to test approximate theories:

(i) Edwards and Taylor[8] evaluate the random phase approximation to find the onset of negative temperature at the energies $e_{\max} = -0.197$ and -0.203, by numerical and steepest descent methods, respectively, compared to $e_{\max} = -0.255 \pm .005$ from Table I for the periodic cell.

(ii) Pointin and Lundgren[10] use mean-field theory to predict the maximum of the probability density for neutral vortices in a box. From their Eq. (43), in our notation,

$$\begin{aligned}(E_N)_{\max} &= -0.154(4\pi) + (1/2)\log N \\ &= \tilde{E} + (1/2)\log 4N + e_{\max}\end{aligned}$$

where the second expression relates N vortices in a box to $4N$ correlated vortices in a periodic cell, as explained in Section 2. Solving for $e_{\max}$ gives $e_{\max} = -1.32$, compared with Table I, $e_{\max} = -1.40 \pm 0.03$.

(iii) The maximum of the probability density for the periodic cell is predicted[9,7] by the random phase approximation to occur at $(E_N)_{\max} = \tilde{E} + (1/2)\log N$, i.e., at $e_{\max} = 0$. But from (2.8), $\langle e \rangle = 0$, and we know from U-statistics that the distribution is skewed. Therefore, it would be unlikely for $\langle e \rangle = e_{\max}$; indeed, $e_{\max} = -0.255 \pm 0.0.005$ from Table I.

(iv) A form of the vortex energy equivalent to (2.2) was obtained by Seyler, who furthermore derived thermodynamics by obtaining an explicit formula for the probability density,[9]

$$\Omega_{\text{rpa}}(e) = \Omega_0 \exp\{1 - 2(e - e_0) - \exp[-2(e - e_0)]\} \tag{5.1}$$

where our notation is used. (Seyler's $e^2/l = 1/2$ here.) This derivation was based on the random phase approximation (rpa) following Taylor.[27] The maximum of $\Omega_{\text{rpa}}(e)$ occurs at e_0, which, according to Seyler, has the value $e_0 = 0$. This value, however, is inconsistent with the fact that $\langle e \rangle = 0$. Shifting e_0 to -0.284 to obtain $\langle e \rangle = \int e\Omega_{\text{rpa}}(e)\, de = 0$ gives much better agreement with the numerical results (that are exact within sampling error). Even so, $\Omega_{\text{rpa}}(e)$ is still too large in the high-energy tail, as seen in Fig. 15, where (5.1) with and without the shift is compared with the numerical estimate of Fig. 1.

By contrast to the statistical theory of vortex systems, the thermodynamic theory is not so well founded—it fails in at least two respects.

First, the formal thermodynamic limit is not uniformly convergent. We showed in Section 2 that the maximum of the probability density occurs at a value of the energy density which increases with N exactly as $\log \sqrt{N}$ (equivalently, $\log \sqrt{A}$). In this sense, there is no negative temperature in the limit $N \to \infty$.[2] However, negative temperature is a ubiquitous feature, being present in any finite vortex system or any infinite lattice with a finite unit cell. Moreover, the negative-temperature region approaches a rigorous limiting form independent of N. Therefore, it is reasonable to preserve negative temperature as $N \to \infty$ by considering thermodynamic functions with respect to $E - \log \sqrt{N}$.

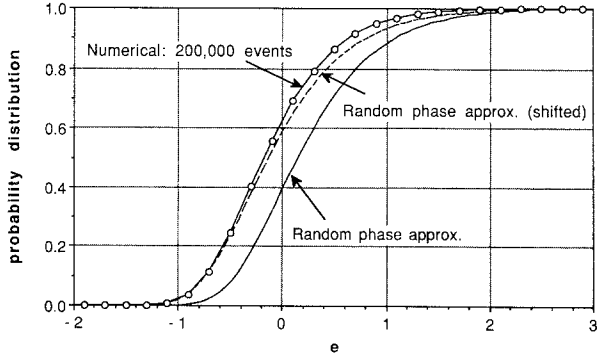

Fig. 15. Numerical distribution function for vortices in a square periodic cell averaged over $N = 20, 40, 80, 160$ (total of 200,000 events) compared with random phase approximation[9] (solid curve) and rpa adjusted to give the correct expected value, $\langle e \rangle = 0$ (dashed curve).

The second failure is more severe and is caused by the argument of the limiting probability density being intrinsic instead of extrinsic. That is, $\Omega_N(\mathscr{E}) \to \Omega(e)$, where $\Omega(e)$ is the function estimated in Figs. 1, 3, and 4 for different cases. As a result, the temperature becomes

$$\frac{1}{T} = \left(\frac{\partial S}{\partial \mathscr{E}}\right)_A = \frac{\kappa_B}{N} \frac{\Omega'(e)}{\Omega(e)} \tag{5.2}$$

which is not intrinsic and, therefore, not thermodynamic, as pointed out years ago by Edwards and Taylor.[8] [These difficulties disappear, of course, with a finite-ranged interaction, such as the modified Bessel function $K_0(r/\lambda)$ appropriate for superconducting vortices.[8]] Note that (5.2) does not rule out the existence of an intrinsic temperature if for some range of T in the interval $0 \leqslant T < \infty$ there exists E for which

$$\lim_{N \to \infty} \frac{\kappa_B}{N} \frac{\Omega'_N(E - \tilde{E} - \log\sqrt{N})}{\Omega_N(E - \tilde{E} - \log\sqrt{N})} = \frac{1}{T} \tag{5.3}$$

If so, then this could be interpreted to mean that, in the thermodynamic limit, there *was* a well-defined intrinsic energy as a function of temperature, $E(T)$. Clearly, such a relation $E(T)$ would also have to depend on the ratio N_+/N because for $N_+/N = 1$ the energy per vortex is bounded below, while for $0 < N_+/N < 1$ the energy per vortex is unbounded below.

The mere existence of a limiting density Ω may determine the relation between E and T in the thermodynamic limit, however. If the convergence in density is sufficiently fast so that Ω_N may be replaced by Ω in (5.3), and if the limit exists for one value of E, then the limit exists for all values and $T(E) = T(0)\exp(2E)$.

Nevertheless, the quantity N/T for vortices in a box appears in the literature as calculated from the sinh-Poisson equation[10] for a nonneutral system and from the random phase approximation[11] for a neutral system. We show N/T in Fig. 16 as obtained from the limiting numerical estimates of $\Omega(e)$ for the periodic cell, neutral box, and box with surface vorticity. The inset shows dimensionless heat capacity at constant area,

$$\frac{C_A}{\kappa_B} = \frac{1}{\kappa_B}\left(\frac{\partial \mathscr{E}}{\partial T}\right)_A = \frac{[\Omega'(e)/\Omega]^2}{[\Omega'(e)/\Omega]^2 - \Omega''(e)/\Omega} \tag{5.4}$$

for the periodic cell and neutral box. There is no anomalous N dependence in the heat capacity.

Our N/T for the neutral box agrees qualitatively with ref. 11, but our exact analysis is *not* consistent with the "sinh-Poisson" values of N/T for the nonneutral box from ref. 10. From (2.16) and (5.2) it is easy to see that

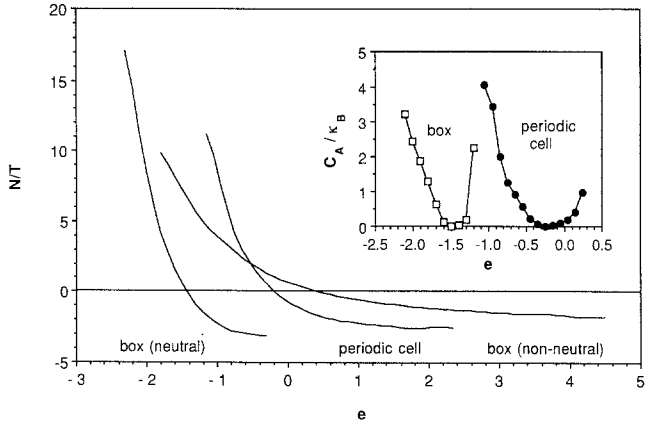

Fig. 16. Inverse dimensionless temperature numerically derived from the limiting distributions in Fig. 1 (periodic cell), Fig. 3 (neutral box), and Fig. 5 (box with perimeter vorticity). The units of $1/T$ are $4\pi\kappa_B/\rho\gamma^2$, where ρ is the fluid mass per unit area and γ is the unit of circulation. Inset: corresponding heat capacities at constant area for the periodic cell and neutral box.

the temperature with respect to e/N (equal within constants to Pointin and Lundgren's $\tilde{E}$) is exactly

$$\frac{N}{T} = -\frac{e/N - (n_+ - n_-)^2 \Gamma^2 \mu/2}{(n_+ - n_-)^2 \Gamma^4 (\langle \mu_i^2 \rangle - \mu^2)} \tag{5.5}$$

unlike Fig. 3 of ref. 10, which shows a highly nonlinear relation between N/T and e/N. Clearly, the sinh-Poisson equation needs to be improved for the nonneutral case.

In view of the thermodynamic failures discussed above, the physical content of the Salzberg–Prager–May equation of state[3,4] may be questioned. This relation follows from the form of the energy in (2.2), which isolates the dependence on A in the logarithm,

$$NE(\mathbf{r}_1, \ldots, \mathbf{r}_N) = N\overline{\Gamma^2}(\tilde{E} + \log\sqrt{A}) + Ne \tag{5.6}$$

The entropy $S(\mathscr{E}, A) = \kappa_B \log[A^N \Omega(\mathscr{E}, A)]$, where the probability density $\Omega(\mathscr{E}, A) = \int \cdots \int dr_1 \cdots dr_N \, \delta(\mathscr{E} - NE)$ involves integration over dimensionless unit squares. The formal equation of state now follows easily from the thermodynamic definition of pressure,

$$P = -\left(\frac{\partial \mathscr{E}}{\partial A}\right)_S = \left(\frac{\partial S}{\partial A}\right)_{\mathscr{E}} \left(\frac{\partial S}{\partial \mathscr{E}}\right)_A^{-1}$$

$$= \frac{N}{A}\left[\kappa_B T - \frac{1}{2}\left(\frac{\rho\gamma^2}{4\pi}\right)\overline{\Gamma^2}\right] \tag{5.7}$$

where we used $\kappa_B T = \Omega(d\Omega/d\mathscr{E})^{-1}$ and inserted the dimensional energy $\rho\gamma^2/4\pi$ for completeness. Note the indifference of this expression to the mixture of vortex signs, to the form of the interaction e, and to the existence of limiting distributions. No compressibility of the underlying fluid is assumed, although (5.6) implicitly assumes the background density changes with A to maintain overall neutrality. The need to distinguish between the above "pressure" and the conventional pressure of systems with mass is emphasized by Kraichnan and Montgomery.[5]

Although the (more probable) statistical properties as a function of e of the vortex system are effectively the same for $N > 20$, the appearance of the system is decidedly not. In particular, the tendency of vortices to separate into clusters of like sign on the scale of the periodic cell is strongly N-dependent. Evidence points to the average energy $\zeta_N(e)$ between vortices of opposite sign being a function of e/N (Figs. 6 and 7). That is, macroscopic separation of opposite-sign vortices, often identified as the hallmark of negative temperatures, asymptotically disappears as $1/N$ for fixed e. Conversely, for any fixed N, macroscopic separation will occur at sufficiently large e, and the shape of the unit cell influences the probability of finding the two opposite-sign clusters in a particular position (Fig. 8). The existence of *two* separated clusters at high energy only occurs with high probability for neutral systems. Such cluster pairs are still not equivalent to two vortices with circulations $\pm N\Gamma/2$; cf. (3.11).

Asymptotic cluster behavior at large energy is easily derived by noting that the phase space volume $\overline{\Phi_N}(\mathscr{E})$ for $\pm$ vortex clusters of radii $r_\pm$ (normalized to L) having energy greater than $\mathscr{E}$ is $\overline{\Phi_N}(\mathscr{E}) \approx r_+^{2N_+} r_-^{2N_-}$. For sufficiently small clusters the presence of both the periodic boundaries and the intercluster energy may be ignored, giving $\mathscr{E} \approx -N_+^2 \log r_+ - N_-^2 \log r_-$. Solving for r_+ and substituting in $\overline{\Phi_N}$ gives the probability density

$$\Omega_N(\mathscr{E}) = -\frac{d}{d\mathscr{E}} \overline{\Phi_N}(\mathscr{E}) = \frac{2}{N_+} r_-^{2(N_+ - N_-)N_-/N_+} \exp(-2\mathscr{E}/N_+) \qquad (5.8)$$

If $N_+ > N_-$, the probability is maximum when r_- is as large as possible, $r_- \approx 1$, which requires r_+ to be as small as possible. Thus, *only the majority cluster is probable*, and we have the asymptotic form $\Omega_N(e) \sim \exp(-2Ne/N_m)$ and the corresponding temperature $1/T = -8\pi\kappa_B/N_m\rho\gamma^2$, where N_m is the number of the majority species (and we have included dimensional forms). This generalizes a finding of Edwards and Taylor for neutral systems.[8] Whether or not mean-field theories, such as sinh-Poisson, can predict preferential clustering for the majority species remains to be seen. To avoid misunderstanding, we should emphasize that the apparent paradox of T depending on the mixture of vortex signs while the limiting distribution is

rigorously independent of both signs (and strengths) occurs because we considered properties of the high-energy tail of the probability density for finite N. The vanishing tails of finite-N distributions at asymptotic high and low energies can differ from the limiting distribution. Nevertheless, we find that all sufficiently resolved models give a consistent prediction of certain features of the continuous evolution, based on a statistical argument.

One obstacle to the validity of point vortex models of continuous fluid is that the continuous fluid has many more conserved quantities, related to the vorticity distribution, than does the model. A possible explanation for the consistency of the data in Fig. 7 may lie in a statistical theory recently put forward by Miller.[21] In this theory, the continuous vorticity distribution is modeled by a sequence of point vortex configurations which lie on a lattice; the canonical partition function then converges to a limit (at least in the case of zero temperature) as the lattice becomes infinitely fine. In other words, the continuous system is modeled by a sequence of increasingly resolved discrete systems, as in the discussion in Section 3. Miller finds that the only quantity conserved at equilibrium on macroscopic scales is the total vorticity (also conserved by point vortex systems). Further, the equilibrium configuration is that which maximizes the energy, given the observed macroscopic vorticity distribution. This is consistent with the "selective decay" theories proposed by Montgomery and others. Such configurations have been investigated numerically (under periodic boundary conditions) by Carnevale and Vallis,[22] who find them invariably to be two clusters. Thus, Miller's findings, based on the canonical distribution, are consistent with ours based on the microcanonical.

The decay of high-Reynolds-number flow in two dimensions contains generic features that are statistical phenomena—not only is the final state of well-separated clusters achieved by a purely random walk, but intermediate-state properties also bear a reasonable resemblance to integration results. Moreover, the relative number of random steps necessary to pass through the various stages correlates well with dynamical times. We estimate that the computation time required to statistically evolve the vortex model is less than 10^{-4} of that required using direct integration of the dynamical equations at comparable resolution. Of course, other features of the decay, such as the tendrils accompanying the dynamic merger of vorticity regions, lie outside this treatment based on relative phase volume.

The decay of the vortex system (through viscous loss of $+-$ pairs) reduces the available phase space, as does the decay of all dynamical systems. Once the vortex system enters the negative-temperature region, the contraction of phase space drives the system to even higher energy density (energy per vortex), necessarily resulting in the emergence of coherent flow structure (vortex clusters) from an initial state of randomly distributed

vorticity. Thus, the "particle-like behavior of the vorticity" referred to by Matthaeus *et al.*[26] has a natural interpretation in the statistical vortex model of relaxation. The fact that a rigorous limiting distribution underlies the phase space probability as a function of energy density justifies the implicit modeling assumption of uniform and generic statistical behavior as N decreases (so long as $N > 20$). Onsager's mechanism, coupled with the viscous annihilation of proximate and opposite vorticities, explains the appearance of well-defined vortices in a fluid where the vorticity is smoothly spread out initially.

It should not be surprising that negative temperatures have a strong relation to flow states, especially those at high Reynolds number. As noted by others, the high-grade energy represented by flow is not thermodynamic, i.e., it is induced not by contact with a heat bath, but by mechanical force. Like the decay of other systems having nonthermodynamic states (e.g., inversions of excitation populations), the decay of high-Reynolds-number flow can pass through unexpected intermediate states having coherent structure (as inverted populations of atomic levels can generate coherent electromagnetic waves).

ACKNOWLEDGMENTS

It is a pleasure to acknowledge discussions with K. Campbell, Y. Kimura, D. Montgomery, J. Palmore, R. Redner, and L. Turner. K. O'N. wishes also to thank the Center for Nonlinear Studies at Los Alamos for travel support. An abbreviated version of this work was first presented at the NATO workshop, Nonlinear Dynamical Structures in Simple and Complex Liquids, Los Alamos National Laboratory (CNLS), June 26–29, 1990, directed by Lui Lam, whom we wish to thank for his interest.

REFERENCES

1. L. Onsager, Statistical hydrodynamics, *Nuovo Cimento (Suppl.)* **6**:279–287 (1949).
2. J. Fröhlich and D. Ruelle, Statistical mechanics of vortices in an inviscid two-dimensional fluid, *Commun. Math. Phys.* **87**:1–36 (1982).
3. E. H. Hauge and P. C. Hemmer, The two-dimensional Coulomb gas, *Phys. Norveg.* **5**:209–217 (1971).
4. Y. B. Pointin and T. S. Lundgren, Equation of state of a vortex fluid, *Phys. Rev. A* **13**:1274–1275 (1976).
5. R. H. Kraichnan and D. Montgomery, Two-dimensional turbulence, *Rep. Prog. Phys.* **43**:547–619 (1980).
6. D. Montgomery, Two-dimensional vortex motion and negative temperatures, *Phys. Lett.* **39A**:7–8 (1972).
7. D. Montgomery and G. Joyce, Statistical mechanics of 'negative temperature' states, *Phys. Fluids* **17**:1139–1145 (1974).

8. S. F. Edwards and J. B. Taylor, Negative temperature states of two-dimensional plasmas and vortex fluids, *Proc. R. Soc. Lond. A* **336**:257–271 (1974).
9. C. E. Seyler, Jr., Thermodynamics of two-dimensional plasmas or discrete line vortex fluids, *Phys. Fluids* **19**:1336–1341 (1976).
10. Y. B. Pointin and T. S. Lundgren, Statistical mechanics of two-dimensional vortices in a bounded container, *Phys. Fluids* **19**:1459–1470 (1976).
11. T. S. Lundgren and Y. B. Pointin, Non-Gaussian probability distributions for a vortex fluid, *Phys. Fluids* **20**:356–363 (1977).
12. T. S. Lundgren and Y. B. Pointin, Statistical mechanics of two-dimensional vortices, *J. Stat. Phys.* **17**:323–355 (1977).
13. J. L. Lebowitz and E. H. Lieb, Existence of thermodynamics for real matter, *Phys. Rev. Lett.* **22**:631–634 (1969); E. H. Lieb and J. L. Lebowitz, The constitution of matter: Existence of thermodynamics for systems composed of electrons and nuclei, *Adv. Math.* **9**:316–398 (1972).
14. K. A. O'Neil, The energy of a vortex lattice configuration, in *Mathematical Aspects of Vortex Dynamics*, R. E. Caflisch, ed. (Society for Industrial and Applied Mathematics, Philadelphia, 1988), pp. 217–220.
15. L. J. Campbell, M. M. Doria, and J. B. Kadtke, Energy of infinite vortex lattices, *Phys. Rev. A* **39**:5436–5439 (1989); L. J. Campbell, Vortex lattices in theory and practice, in *Mathematical Aspects of Vortex Dynamics*, R. E. Caflisch, ed. (Society for Industrial and Applied Mathematics, Philadelphia, 1988), pp. 195–204.
16. K. A. O'Neil and R. A. Redner, On the limiting distribution of pair-summable potential functions in many particle systems, *J. Stat. Phys.* **62** (1991), to be published.
17. R. L. Serfling, *Approximation Theorems of Mathematical Statistics* (Wiley, New York, 1980), esp. Chapter V.
18. V. Penna, Dynamics and spectral properties of a quantum 2d bounded vortex system, *Physica A* **152**:400–419 (1988).
19. A. C. Ting, H. H. Chen, and Y. C. Lee, Exact vortex solutions of two-dimensional guiding-center plasmas, *Phys. Rev. Lett.* **53**:1348–1351 (1984).
20. J. Goodman, T. Y. Hou, and J. Lowengrub, Convergence of the point vortex method for the 2-D Euler equations, *Commun. Pure Appl. Math.* **43**:415–430 (1990).
21. J. Miller, Statistical mechanics of Euler equations in two dimensions, *Phys. Rev. Lett.* **65**:2137–2140 (1990).
22. G. F. Carnevale and G. K. Vallis, Pseudo-advective relaxation to stable states of inviscid two-dimensional fluids, *J. Fluid Mech.* **213**:549–571 (1990).
23. A. J. Chorin, Numerical study of slightly viscous flow, *J. Fluid Mech.* **57**:785–796 (1973).
24. J. B. Weiss and J. C. McWilliams, Non-ergodicity of point vortices, *Phys. Fluids A* **3**:835–844 (1991).
25. J. C. McWilliams, The emergence of isolated coherent vortices in turbulent flow, *J. Fluid Mech.* **146**:21–43 (1984).
26. W. H. Matthaeus, W. T. Stribling, D. Martinez, S. Oughton, and D. Montgomery, Selective decay and coherent vortices in two-dimensional incompressible turbulence, *Phys. Rev. Lett.* **66**:2731–2734 (1991).
27. J. B. Taylor, Negative temperatures in two dimensional vortex motion, *Phys. Lett.* **40A**:1–2 (1972).